Proceedings of DETC'02
ASME 2002 Design Engineering Technical Conferences
and Computer and Information in Engineering Conference
Montreal, Canada, September 29-October 2, 2002

DETC2002/DAC-34083

DECOMPOSITION-BASED ASSEMBLY SYNTHESIS BASED ON STRUCTURAL STIFFNESS CONSIDERATIONS

Naesung Lyu and **Kazuhiro Saitou***
Department of Mechanical Engineering
University of Michigan
Ann Arbor, MI 48109-2125, USA
E-mail:{nlyu,kazu}@umich.edu

ABSTRACT

This paper presents a method for systematically decomposes product geometry into a set of components considering the structural stiffness of the end product. A structure is represented a graph of its topology, and the optimal decomposition is obtained by combining FEM analyses with a Genetic Algorithm. As a case study, the side frame of a passenger car is decomposed for the minimum distortion of the front door panel geometry, where spot-welded joints are modeled as torsional springs. First, the rates of the torsional springs are treated as constant values obtained in the literature. Second, they are treated as design variables within realistic bounds. By allowing the change in the joint rates, it is demonstrated that the optimal decomposition can achieve the smaller distortion with less amount of joint stiffness (hence less welding spots), than the optimal decomposition with the typical joint rates available in the literature.

INTRODUCTION

To design any structural product, engineers adopt one of the two design methods: top-down and bottom-up methods. As the end products become more complicated and highly integrated, the top-down method is preferred since it allows the easier design assessment of an entire product during the design process. Top-down methods typically start with the preliminary design of the overall end product structure and proceed with the detailed design of components and substructures. If geometries and desired functions are simple, the structure can be built in one piece. To build complex structures in one piece, however, engineers need sophisticated manufacturing methods that would likely result in the higher manufacturing cost. Also, one piece structure will suffer from the lack of modularity: it would require the change or replacement of the entire structure even for local design changes or failures. It would be often natural, therefore, to design a structural product as an assembly of components with simpler geometries.

To design multi-component structural products in top-down fashion, an overall product geometry must be decomposed at some point during the design process. In industry, such decompositions are typically done prior to the detailed design of individual components, taking into account of geometry, functionality, and manufacturability issues. However, this process is usually non-systematic and hence might result in a decomposition overlooking the integrity of the end product. For instance, automotive industry utilizes a handful of basic decomposition schemes of a vehicle that have not been changed for decades. This is because the desired form, functionality, materials, joining methods, and weight distribution of mass-production vehicles have not changed much for decades. However, the conventional decomposition schemes may no longer be valid for the vehicles with new technologies such as space frame, lightweight materials, and fuel cell or battery powered motors, which would have dramatically different structural properties, weight distribution, and packaging requirements. This motivates the development of a systematic decomposition methodology presented in this paper.

In our previous work (Saitou and Yetis, 2000; Yetis and Saitou, 2000; Cetin and Saitou, 2001), we have termed *assembly synthesis* as the decision of which component set can achieve a desired function of the end product when assembled together, and assembly synthesis is achieved by the decomposition of product geometry. Since assembly process generally accounts

* corresponding author

for more than 50% of manufacturing costs and also affects the product quality (Lotter, 1989), assembly synthesis would have a large impact on the quality and cost of the end product.

As an extension of our previous work, this paper introduces a method for decomposing a product geometry considering the structural stiffness of the end product. Because the decomposition will determine the location of the joints between components, the structural integrity (*e.g*., stiffness) of the end-product will be heavily influenced by the choice of a particular decomposition. Designers can use this method to get feedback on the possible decompositions before the detailed design stage. Via the decomposition of a graph representing its topology, a product is decomposed into a candidate set of components with simpler geometries, where joints among components are modeled as torsional springs. By combining FEM analyses with Genetic Algorithms (Holland, 1975; Goldberg, 1989), the optimal decomposition that gives the desired structural property of the end product is obtained. The case study discusses the assembly synthesis of the automotive side door panels.

RELATED WORK

Design for assembly and assembly sequence design

Many attempts have been made on assembly design and planning for decades. Among them, Boothroyd and Dewhurst (1983) are widely regarded as major contributors in the formalization of design for assembly (DFA) concept. In their method (Boothroyd *et al.*, 1994), assembly costs are first reduced by the reduction of part count, followed by the local design changes of the remaining parts to enhance their assembleability and manufacturability. This basic approach is adopted by most subsequent works on DFA. There are a number of researchers investigating the integration of DFA and assembly sequence planning (De Fanzio and Whitney, 1987; Ko and Lee, 1987), where assembly sequence planning is proposed as the enumeration of geometrically feasible cut-sets of a liaison graph, an undirected graph representing the connectivity among components in an assembly. The local design changes are made to the components to improve the quality of the best assembly sequence. These works, however, focus on the local design changes of a given assembly design (*i.e*., already "decomposed" product design), and have less emphasis on *how to synthesize* an assembly to start with.

Automotive body structure modeling

In automotive body structure, high stiffness is one of the most important design factors, since it is directly related the improved ride and NVH (Noise, Vibration, and Harshness) qualities and crashworthiness (Ashley, 1997). To accurately predict the stiffness of an assembled body structure, Chang (1974) modeled spot-welded joints as torsional springs, and demonstrated that the model can accurately predict the global deformation of automotive body substructures. Recently, correlation between torsional spring properties of joints and the length of structural member was studied (Lee & Nikolaidis, 1998) to assess the accuracy of joint model. However, these works focus on the accurate prediction of the structural behavior of a given assembly (*i.e*., already "decomposed" structure design) and do not address *where to place joints* based on the predicted stiffness of an assembly.

APPROACH

This section describes the proposed method for simultaneously identifying the optimal set of components and joint attributes (rates of torsional springs) considering the stiffness of the assembled structure. It is assumed that joints have less stiffness than components and therefore reduce the rigidity of the overall structure[1]. The following steps outline the basic procedure:

1. Given a structure of interest (Figure 1 (a)), define the basic members and potential joint locations (Figure 1 (b)).
2. Construct a *structural topology graph* $G = (V, E)$ with node set V and edge set E, which represents the connectivity of the basic members defined in step 1 (Figure 1 (c)). A node and an edge in G correspond to a member and a joint, respectively.
3. Obtain the optimal decomposition of G that gives the best structural performance via Genetic Algorithm (Figure 1 (d)), and map the decomposition result back to the original structure (Figure 1 (e)). During optimization, the structural performance of decomposition is evaluated by a Finite Element Method.

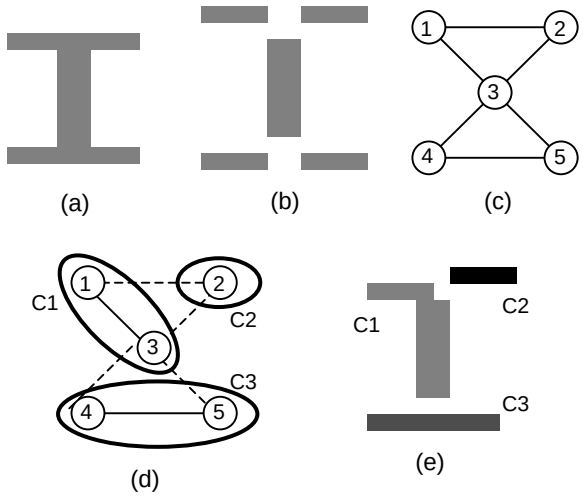

Figure 1. Outline of the decomposition procedure. (a) structure to be decomposed, (b) basic members and potential joint locations, (c) structural topology graph *G*, (d) optimal decomposition of *G*, and (e) resulting decomposition of the original structure.

[1] While this is true for many joints such as spot welds, threaded fasteners, and rivets, some joints (*eg*., arc welds) can be stiffer than components themselves.

Definition of design variables

Since a graph can be decomposed by deleting some edges, a vector $\boldsymbol{x} = (x_i)$ of binary variable x_i can be used to represent a decomposition of structural topology graph *G*. The dimension of the vector $\boldsymbol{x} = (x_i)$ is equal to the number of the edges |*E*| in *G*:

$$\boldsymbol{x} = \left(x_1\ x_2 \cdots x_i \cdots x_{|E|-1}\ x_{|E|}\right) \tag{1}$$

where

$$x_i = \begin{cases} 1 \text{ if } e_i \text{ exists in the decomposed graph} \\ 0 \text{ otherwise} \end{cases}$$

Figure 2 illustrates example decompositions of a graph and the corresponding values of vector ***x***. Figure 2 (a) shows the original graph *G* without decomposition, where $V = \{n_1, n_2, n_3\}$ and $E = \{e_1, e_2, e_3\}$. Since all edges are present without decomposition, the corresponding vector $\boldsymbol{x} = (x_1, x_2, x_3) = (1, 1, 1)$. If vector x takes this value, an entire graph *G* is interpreted as one component, which is denoted as c_1 in the figure. Similarly, Figure 2 (b) shows a two-component decomposition consisting of components c_1 and c_2 obtained by deleting e_1 and e_2 (indicated as dashed lines) in *G*. This decomposition can be represented using vector ***x*** as $\boldsymbol{x} = (x_1, x_2, x_3) = (0, 0, 1)$.

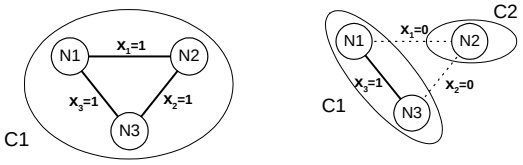

(a) (b)

Figure 2. Example decompositions of a graph and the corresponding values of vector *x*. (a) the original graph with *x* = (1, 1, 1), and (b) two component decomposition with *x* = (0, 0, 1).

Joint attributes are defined as another vector $\boldsymbol{y} = (y_i)$ of positive number $y_i \in \mathbf{R}$. In the following case studies, the element y_i represents the rates (spring constant) of torsional springs [Nm/rad] of the joint corresponding to edge e_i of the structural topology graph. During optimization, the value of y_i is ignored if $x_i = 0$.

Definition of constraints

The first constraint for the design variable ***x*** comes from the definition of ***x***. Namely, each element of the vector ***x*** should be 0 or 1:

$$x_i \in \{0,1\} \tag{2}$$

In the current formulation, we assume a desired number of decomposition *k* is given by the designer. Therefore, the decomposition of *G* should result in *k* disconnected subgraphs:

$$\texttt{N\_COMPONENTS}(\texttt{GRAPH}(\boldsymbol{x})) = k \tag{3}$$

where $\texttt{GRAPH}(\boldsymbol{x})$ is a function that returns the graph corresponding to the decomposition of *G* with ***x***, and $\texttt{N\_COMPONENTS}(G)$ is a function that returns the number of disconnected subgraphs ("components") in graph *G*.

The third constraint of ***x*** is to ensure the decomposed components are economically manufacturable by given manufacturing means. For example, components with a branched topology would not be economically manufacturable by sheet metal stamping. Also, when we considering 3D structure with stamping process, any decomposed component should be in 2 dimensional plane. The following is a general form of manufacturability constraint:

$$\texttt{IS\_MANUFACTURABLE}(\texttt{GRAPH}(\mathbf{x})) = 1 \tag{4}$$

where $\texttt{IS\_MANUFACTURABLE}(G)$ is a function that returns 1 when all disconnected subgraphs in *G* are manufacturable by given manufacturing methods, such as stamping of sheet metal, and otherwise returns 0. Explicit expression of this constraint includes routines checking the geometry of the given decomposed components if it has branched topology or not.

Finally, elements of ***y*** should simply be among the feasible selections:

$$y_i \in F \tag{5}$$

where *F* is a set of feasible values of given joint attributes (rate of torsional spring in the following example).

Definition of objective function

A component set specified by vector ***x*** (a set of the node sets of disconnected subgraphs in $\texttt{GRAPH}(\boldsymbol{x})$) is evaluated for the stiffness of the assembled structure with the joint attribute specified by ***y***. The stiffness of an assembled structure can be measured as the negative of the sum of displacements at the pre-specified points of the structure for given boundary conditions:

$$\textit{stiffness} = -\texttt{DISPLACEMENTS}(\texttt{GRAPH}(\boldsymbol{x}), \boldsymbol{y}) \tag{6}$$

where $\texttt{DISPLACEMENTS}(G, \boldsymbol{y})$ is a function that returns the sum (or the maximum) of displacements at the pre-specified points of the assembled structure, computed by Finite Element Methods.

Since we assume the number of components is given, a decomposition would be the stiffest if the maximum spring constant is used at all joints. This corresponds to the situation where the maximum number of spot welds is used for all joints, which is obviously not a very economical solution. It would be of engineering interest, therefore, to find out the optimal balance between the sum of spring constants (a measure of the total number of spot welds) and structural stiffness of the assemble structure. This results in the following objective function (to be maximized) that evaluates stiffness of the structure and also total sum of spring constants in the joints:

$$f(\boldsymbol{x},\boldsymbol{y}) \;=\; C + w_1 \cdot \mathit{stiffness} - w_2 \cdot \sum y_i \qquad (7)$$

where C is a positive constant, *stiffness* is defined as Equation (6), w_1 and w_2 are positive weights. The purpose of constant C is to ensure the positive value of *fitness* for any values of $\boldsymbol{x}$ and $\boldsymbol{y}$, required by Genetic Algorithms as stated below. After all, the following optimization model is to be solved:

maximize $f(\boldsymbol{x},\boldsymbol{y})$ (objective function in Equation (7))

subject to

$$\mathtt{N\_COMPONENTS(GRAPH(}\boldsymbol{x}\mathtt{))} = k$$
$$\mathtt{IS\_MANUFACTURABLE(GRAPH(}\boldsymbol{x}\mathtt{))} = 1$$
$$\boldsymbol{x} = (x_i),\quad x_i \in \{0,1\},\quad i = 1\cdots|E|$$
$$\boldsymbol{y} = (y_i),\quad y_i \in F,\ i = 1\cdots|E|$$

It should be noted that the above optimization model contains a standard k-partitioning problem of an undirected graph (Garey and Johnson, 1979), and additional nonlinear terms in the objective functions and constraints.

Genetic Algorithms

Due to the NP-completeness of the underlying graph partitioning problem (Garey and Johnson, 1979) the above optimization model is solved using Genetic Algorithm (GA). GA is a heuristic optimization algorithm that simulates the process of natural selection in biological evolution (Holland, 1975; Goldberg, 1989). The results of the following examples are obtained using a steady-state GA (Davis, 1991), a variation of the "vanilla" GA tailored to prevent premature convergence. Basic steps of a steady-state GA is outlined below (Yetis and Saitou, 2000):

1. Randomly create a population P of n individuals with chromosomes (a representation of design variable $\boldsymbol{x}$). Evaluate their fitness values and store the best chromosome. Also create an empty subpopulation Q.
2. Select two chromosomes c_i and c_j in P with probability:

$$\text{Prob}(c_i \text{ is selected}) = \frac{f_i}{\sum f_k}$$

where f_i is the fitness value of chromosome c_i.

3. Crossover c_i and c_j to generate two new chromosomes c_i' and c_j'.
4. Mutate c_i' and c_j' with a certain low probability.
5. Evaluate the fitness values of c_i' and c_j'. Add them in Q. If Q contains less than m new chromosomes, go to step 2.
6. Replace m chromosome in P with m chromosomes in Q. Empty Q. Update the best chromosome and increase the generation counter. If the generation counter has reached a pre-specified number, terminate the process and return the best chromosome. Otherwise go to step 2.

In GAs, design variables are represented as a "string" of numbers called chromosomes on which genetic operators such as crossover and mutation are performed. The components of our two design variables $\boldsymbol{x} = (x_i)$ and $\boldsymbol{y} = (y_i)$ are simply lay out as $x_1, x_2, \ldots, x_{|E|}, y_1, y_2, \ldots, y_{|E|}$ in a linear chromosome of length $2|E|$ as illustrated in Figure 3.

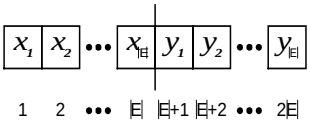

Figure 3. Chromosome representation of design variables $\boldsymbol{x}$ and $\boldsymbol{y}$, where the elements of these vectors are simply laid out to form a linear chromosome of length $2|E|$.

Since we have formulated the optimization model as a maximization problem, the fitness values of a chromosome can be computed from the corresponding values of the design variables $\boldsymbol{x}$ and $\boldsymbol{y}$ as:

$$\mathit{fitness} = f(\boldsymbol{x},\boldsymbol{y}) - \mathit{penalty} \qquad (8)$$

where *penalty* is defined as:

$$\mathit{penalty} = \qquad (9)$$
$$w_3\left(\mathtt{N\_COMPONENTS(GRAPH(}\boldsymbol{x}\mathtt{))} - k\right)^2$$
$$+ w_4\left(\mathtt{IS\_MANUFACTURABLE(GRAPH(}\boldsymbol{x}\mathtt{))} - 1\right)^2$$

were w_3, w_4 are positive weights. After all, the fitness function looks like:

$$
\begin{aligned}
\textit{fitness} = \quad & C - w_1 \cdot \texttt{DISPLACEMENTS}(\texttt{GRAPH}(\boldsymbol{x}), \boldsymbol{y}) \\
& - w_2 \cdot \sum y_i \\
& - w_3 \left(\texttt{N\_COMPONENTS}(\texttt{GRAPH}(\boldsymbol{x})) - k\right)^2 \\
& - w_4 \left(\texttt{IS\_MANUFACTURABLE}(\texttt{GRAPH}(\boldsymbol{x})) - 1\right)^2
\end{aligned} \tag{10}
$$

As stated earlier, computing DISPLACEMENTS(G,$\boldsymbol{y}$) requires Finite Element Methods and is the most time consuming part among the above four terms in the fitness function. To improve the runtime efficiency, we have devised a database to store each FEM result with the corresponding value of chromosome during a GA run. When a chromosome is evaluated, the algorithm first looks into the datable for the same chromosome value. If there is a match, it simply retrieves the pre-computed FEM result and skips the FEM analysis.

CASE STUDIES

In this section, the assembly synthesis method described in the previous section is applied to a side frame of a four-door sedan type passenger car (Figure 4). The following assumptions are made according to (Chang, 1974): 1) the side frame is subject to a static bending due to weight of the vehicle, 2) the frame can be modeled as a two dimensional structure, and 3) its components are joined with spot welds modeled as torsional springs, whose axis of rotation is perpendicular to the plane on which the frame lies.

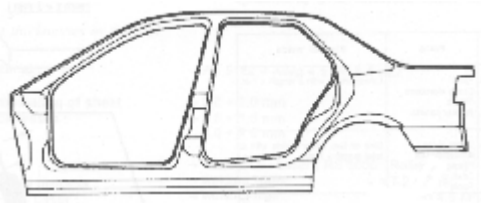

Figure 4. A side frame of a passenger car used in case studies.

Structural model

Figures 5 and 6 show the 9 basic members defined on the side frame in Figure 4, and the resulting structural topology graph, respectively. Each basic member was modeled as a beam element with a constant cross section, whose properties (area and moment of inertia) are listed in Table 1, which are calculated from the body geometry of a typical passenger car. Each intersecting member in the frame is assumed to be of constant cross section up to the intersection of the axis of the members. This will reduce the connection among multiple beams to be represented as a point (Chang, 1974), and hence allows to model a joint as a torsional spring around the point.

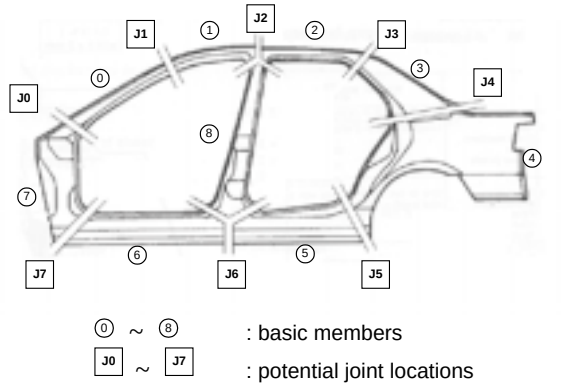

Figure 5. Definition of basic members and potential joint locations of side frame structure.

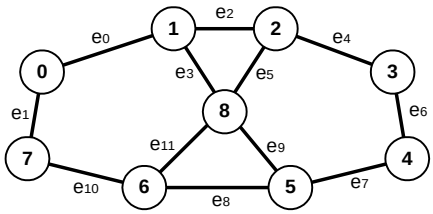

Figure 6. Structural topology graph of the side frame, with nodes 0 ~ 7 represent basic members, and edge e1 ~ e11 represent potential joints between two basic members.

Table 1. Cross-sectional properties of basic members in Figure 5, calculated from typical body geometry.

No.	Nomenclature	Cross-sectional area [m^2]	Moment of inertia [m^4]
0	Windshield Pillar	3.855×10^{-4}	1.860×10^{-7}
1	Front Roof Rail	4.789×10^{-4}	5.411×10^{-7}
2	Rear Roof Rail	4.789×10^{-4}	5.411×10^{-7}
3	C Pillar	12.840×10^{-4}	9.967×10^{-7}
4	Rear Weal House	7.840×10^{-4}	9.342×10^{-7}
5	Rear Rocker	20.730×10^{-4}	8.792×10^{-7}
6	Front Rocker	20.730×10^{-4}	8.792×10^{-7}
7	Hinge Pillar	10.369×10^{-4}	12.784×10^{-7}
8	Center Pillar	5.443×10^{-4}	1.625×10^{-7}

Due to the complex geometry, residual stresses, and friction between the mating surfaces, the detailed structural modeling of spot welded joints are quite difficult (Chang, 1974). It is a standard industry practice, therefore, to model spot-welded joints as torsional springs, whose spring rates [Nm/rad] are empirically obtained though experiments or detailed FEM analyses. In the following case studies, the rates of the torsional

springs at each joint in a decomposition (vector $\boldsymbol{y}$ in Equation (10)) are regarded as:

- **Case 1:** constants in Table 2.
- **Case 2:** variables between 0.01×10^6 and 0.20×10^6 [Nm/rad].

In other words, in Case 1 vector $\boldsymbol{x}$ in Equation (10) is the only design variable and vector $\boldsymbol{y}$ is treated as a constant, whereas in Case 2 both $\boldsymbol{x}$ and $\boldsymbol{y}$ are design variables. Since the set of feasible spring rate $F = \{y \mid 0.01\times10^6 \le y \le 0.20\times10^6\}$ in Case 2 contains all values in Table 2, the optimization model (10) in Case 2 is a *relaxation* of the one in Case 1.

Table 2. Torsional spring rates of the joints in side frame of a passenger car (Malen and Kikuchi, 1998).

No.	Joint location	Joint rate [Nm/rad]
J0	Hinge Pillar and Windshield Pillar	0.20×10^6
J1	Windshield Pillar and Front Roof Rail	0.01×10^6
J2	Front and Rear Roof Rails, and Center Pillar	0.01×10^6
J3	Rear Roof Rail and C Pillar	0.01×10^6
J4	C Pillar and Rear Weal House	0.20×10^6
J5	Rear Weal House and Rear Rocker	0.20×10^6
J6	Front Rocker, Rear Rocker and Center Pillar	0.20×10^6
J7	Hinge Pillar and Front Rocker	0.20×10^6

Boundary conditions

The structure was assumed to be placed on a simple support system consisting of a pair of hinge supports at the front body mount location and a pair of roller supports at the mount locations near the rear locker pillar as shown in Figure 7. The loading condition of the static bending strength requirement is considered, where the downward loading is the weight of a passenger car (10,000 [N]).

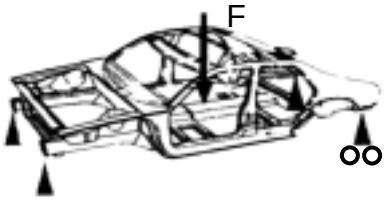

Figure 7. Loading condition of basic bending requirement. Loading F is the weight of a passenger car (10,000 [N]).

Measure of structural stiffness

Under normal loading conditions, the front door frame should retain its original shape to guarantee the normal door opening and closing. Based on this consideration, $\texttt{DISPLACEMENTS}(G, \boldsymbol{y})$ in Equation (10) is defined as:

$$\texttt{DISPLACEMENTS}(G, \boldsymbol{y}) = \max\{\overline{A1A2}, \overline{B1B2}\} \qquad (11)$$

where

A1 = upper right corner of the front *door frame* after deformation.
A2 = upper right corner of the front *door* without deformation, attached to the deformed hinge.
B1 = lower right corner of the front *door frame* after deformation.
B2 = lower right corner of the front *door* without deformation, attached to the deformed hinge.

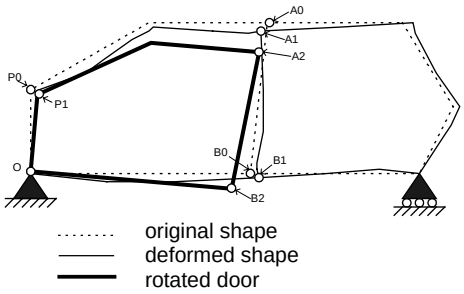

Figure 8. Definition of $\texttt{DISPLACEMENTS}(G, \boldsymbol{y})$ used in case studies. Overall displacement of side frame is max{d_1, d_2}, where d_1 and d_2 are the displacements of upper and lower right corners of the door, respectively, measured with respect to undeformed door geometry attached to deformed hinge OP1.

Points A1, A2, B1, and B2 are illustrated in Figure 8. The locations of A1 and B1 are obtained directly from the FEM results. The following assumptions are made on the locations of A2 and B2:

- The door only rotates around a point O in Figure 8. The angle of rotation is defined as the angle between $\overline{OP0}$ and $\overline{OP1}$. $\overline{OP1}$ represents the hinge without deformation, whereas $\overline{OP0}$ represents the deformed hinge.
- The front door is a rigid body: Deformation of the door due to the external loading is negligible compared to the one of the frame (*i.e.*, the door is a "rigid body").

Software implementation

Figure 9 shows the flowcharts of the implemented software for optimal decomposition of the side frame. During the fitness calculation (Figure 9 (b)), the software generates the input file for a FEM solver, run the FEM solver, and retrieves the necessary data within the output file. The software is written in

C++ program using LEDA[2] libraries. GAlib[3] and ABAQUS[4] are used as a GA optimizer and a FEM solver, respectively.

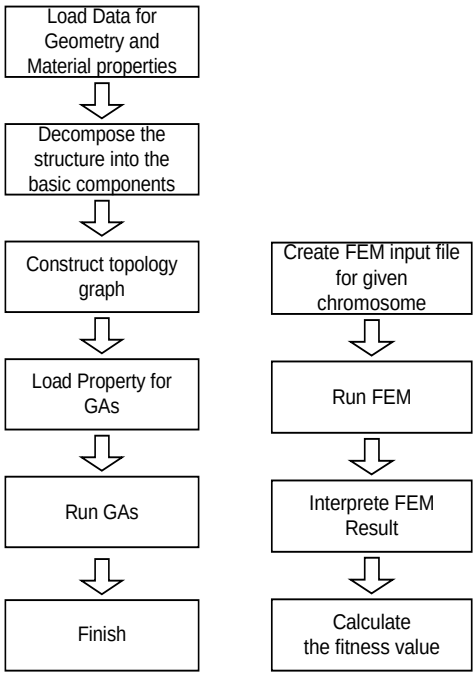

Figure 9. Flowchart of optimal decomposition software. (a) overall flow, and (b) fitness calculation.

Decomposition Results

As a base line for comparing the effect of the joints, we first examined one piece structure with no joints and the fully decomposed structure made of the 9 basic members with the 11 joints defined in Figure 6. The joint rates in Table 2 are used for the FEM analysis of the fully decomposed structure. Since the joints are less stiff than the material of the basic members (sheet iron), it is expected that the fully decomposed structure exhibits a larger value of DISPLACEMENTS(G,y) as defined in Figure 9, than the one piece structure. Figures 10 and 11 show the FEM results of the one-piece structure and the fully-decomposed structure, respectively. As expected, the existence of joints causes a significant increase in the amount of DISPLACEMENTS in the structure, as well as much difference in the deformed shapes. The value of DISPLACEMENTS of the fully decomposed structure (Figure 11) is about 6 times larger than that of the one piece structure (Figure 10). However, even the one piece structure does not fully retain the original shape of the front door, resulted in a fairly large value of DISPLACEMENTS = 1.411 [mm].

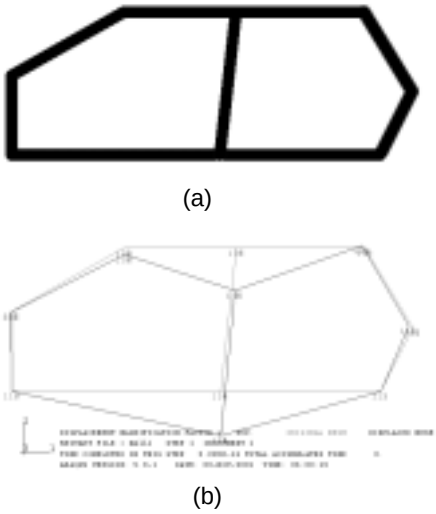

Figure 10. Baseline result. (a) one piece structure and (b) its deformation with DISPLACEMENTS = 1.411 [mm].

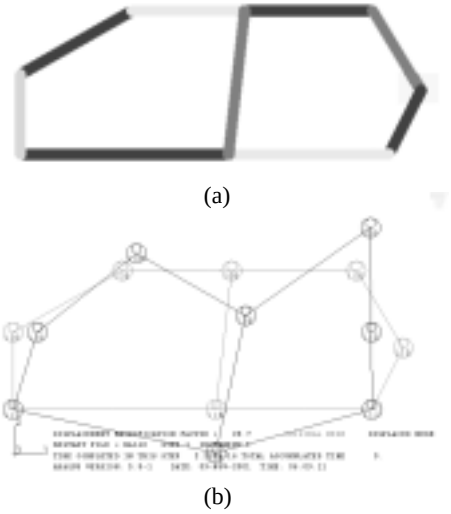

Figure 11. Baseline result. (a) fully decomposed structure and (b) its deformation with DISPLACEMENTS = 8.251 [mm].

Next, the structure is decomposed to 4 and 5 components, each with constant joint rates in Table 2 (Case 1) and variable joint rates between 0.01×10^6 and 0.20×10^6 [Nm/rad] (Case 2). Figures 12 and 13 show the 4- and 5-component optimal decompositions with constant joint rates (Case 1), respectively. Figures 14 and 15 show the 4- and 5-component optimal decompositions with variable joint rates (Case 2), respectively. The following GA parameters are used in these results:

[2] Developed by Algorithmic Solution (http://www.algorithmic-solutions.com).
[3] Developed at MIT by Matt Wall (http://lancet.mit.edu/ga/).
[4] Version 5.8. (http://www.hks.com/).

- number of population = 200.
- number of generation = 100 (Case 1); 200 (Case 2).
- replacement probability = 0.50.
- mutation probability = 0.001 (Case 1); 0.10 (Case 2).
- crossover probability = 0.90.

Table 3 shows a summary of the results of the case studies including the base line cases.

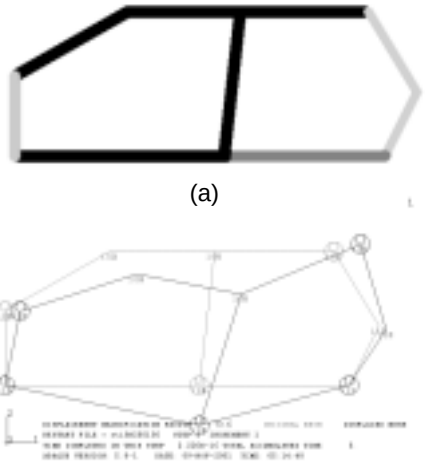

(a)

(b)

Figure 12. 4-component decomposition with constant joint rates in Table 2 (Case 1). (a) optimal decomposition and (b) its deformation with DISPLACEMENTS = 0.075 [mm].

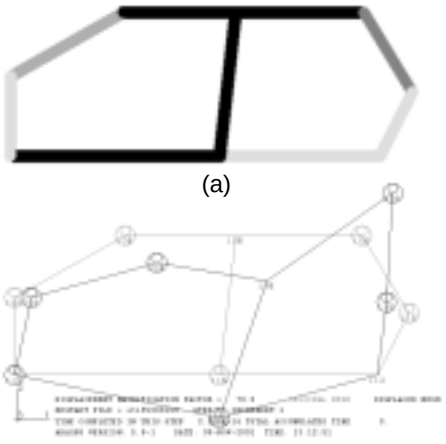

(a)

(b)

Figure 13. 5-component decomposition with constant joint rates in Table 2 (Case 1). (a) optimal decomposition and (b) its deformation with DISPLACEMENTS = 0.109 [mm].

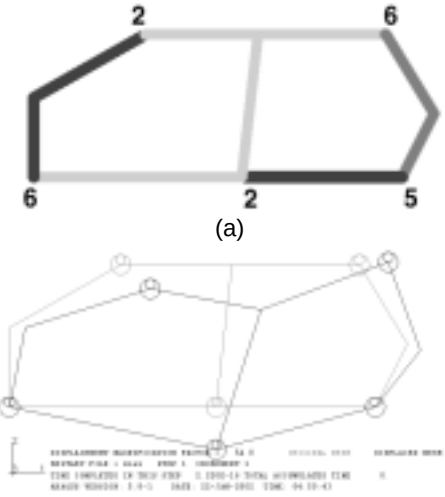

(a)

(b)

Figure 14. 4-component decomposition with variable joint rates (Case 2). (a) optimal decomposition and (b) its deformation with DISPLACEMENTS = 0. 062 [mm]. The number at each joint in (a) indicates the optimal joint rate in [10^4 Nm/rad].

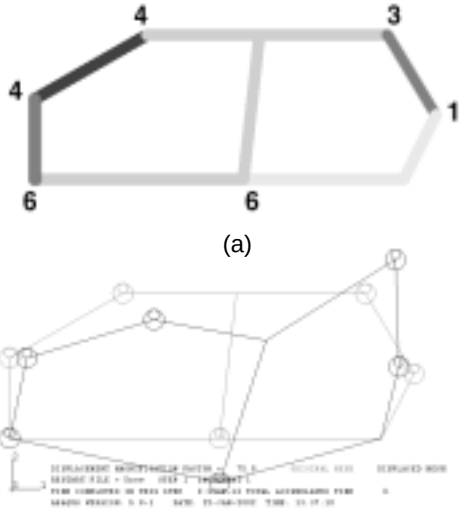

(a)

(b)

Figure 15. 5-component decomposition with variable joint rates. (a) optimal decomposition and (b) its deformation with DISPLACEMENTS = 0. 065 [mm]. The number at each joint in (a) indicates the optimal joint rates in [10^4 Nm/rad].

Table 3. Summary of results. Note that all optimization results produce better DISPLACEMENTS than no decomposition and full decomposition cases. For both k = 4 and 5, Case 2 exhibits better DISPLACEMENTS with less total joint rate (hence less weld spots) than Case 1.

Case	DISPLACEMENTS [mm]	Total joint rate [Nm/rad]
No decomposition (Figure 10)	1.411	0.00×10^6
Full decomposition (Figure 11)	8.251	1.03×10^6
Case 1, k=4 (Figure 12)	0.075	0.81×10^6
Case 1, k=5 (Figure 13)	0.109	0.82×10^6
Case 2, k=4 (Figure 14)	0.062	0.21×10^6
Case 2, k=5 (Figure 15)	0.065	0.24×10^6

The decomposition results in Figures 12 – 15 indicate that the structure is decomposed to a desired number of components and the front door frames after deformation preserve their original shape fairly well. In fact, all 4- and 5- component decompositions resulted in the smaller values of DISPLACEMENTS than the one piece structure in Figure 10. This is due to the fact that rear door frame (basic members 2, 3, 4 and 5) "absorbs" the deformation due to the external loads by having relatively less stiff joints. All the optimized shapes show no joints between Front and Rear Roof Rails (basic members 1 and 2) and Center Pillar (basic member 8) and between Front Rocker (basic member 6) and Center Pillar (basic member 8). These two positions seem to be critical to preserve the shape of the front door frame against the external loads.

Table 3 reveals that Case 2 exhibits smaller DISPLACEMENTS with less total joint rate (hence less weld spots) than Case 1 for both k = 4 and 5. This means, for the same frame design, one can achieve a superior performance (less distortion of the front door frame geometry) with less manufacturing efforts (less number of weld spots). In reality, of course, the distortion of the front door geometry is one of the many criteria which an automotive body structure must satisfy, and hence one cannot simply draw a conclusion that the conventional joints are over designed from these results. As stated earlier, the optimization model of Case 2 is a relaxation of the one of Case 1. Therefore, the optimal solutions of Case 2 must be at least as better as the ones in Case 1, which is shown in Table 3.

SUMMARY AND FUTURE WORK

This paper described a method for optimally decomposing a structural product based on the stiffness of the end product after assembly. A structure is represented a graph of its topology, and the optimal decomposition is obtained by combining FEM analyses with a Genetic Algorithm. As a case study, the side frame of a passenger car is decomposed for the minimum distortion of the front door panel geometry, where spot-welded joints are modeled as torsional springs. First, the rates of the torsional springs are treated as constant values obtained in the literature. Second, they are treated as design variables within realistic bounds. By allowing the change in the joint rates, it is demonstrated that the optimal decomposition can achieve the smaller distortion with less amount of joint stiffness (hence less welding spots), than the optimal decomposition with the typical joint rates available in the literature.

The work presented in this paper is still preliminary and needs extension in many directions. The immediate future work includes the extension of the framework to 3D beam-plate models, the incorporation of other design objective such as global torsion and NVH, and the adoption of more detailed joint models for, *eg.,*. fatigue estimation.

ACKNOWLEDGMENTS

The authors would like to acknowledge the support provided by Toyota Motor Corporation for this research.

REFERENCES

Ashley, S., 1997. "Steel cars face a weighty decision," *Mechanical Engineering*, Vol. 119(2), Feb 1997, pp. 56-61.

Boothroyd, G. and Dewhurst, P., 1983. *Design for Assembly Handbook*, University of Massachusetts, Amherst.

Boothroyd, G., Dewhurst, P., and Winston, K., 1994, *Product Design for Manufacturing and Assembly*, Marcel Dekker, New York.

Bendsøe, M. P. and N. Kikuchi, 1988. "Generating optimal topologies in structural design using a homogenization method," *Computer Methods in Applied Mechanics and Engineering*, Vol. 71, pp. 197-224.

Cetin, O.L. and Saitou, K., 2001. "Decomposition-based assembly synthesis for maximum structural strength and modularity," *Proceedings of the 2001 ASME Design Engineering Technical Conferences*, September 9-12, 2001, Pittsburgh, PA, DETC2001/DAC-21121.

Chang, D., 1974. "Effects of flexible connections on body structural response," *SAE Transactions*, Vol. 83, pp. 233-244.

Davis, L., 1991. *Handbook of Genetic Algorithms*, Van Nostrand Reinhold, New York.

De Fanzio, T., and Whitney, D., 1987. "Simplified generation of all mechanical assembly sequences," *Transaction of IEEE, Journal of Robotics and Automation*, pp.640-658.

Garey, M. R. and Johnson, D. S., 1979. *Computers And Intractability, a Guide to the Theory of NP-completeness*, W. H. Freeman and Company, New York.

Goldberg, D., 1989. *Genetic Algorithms in Search, Optimization, and Machine Learning*, Addison-Wesley, Reading, Massachusetts.

Holland, J., 1975. *Adaptation in Natural and Artificial Systems*, University of Michigan Press, Ann Arbor, Michigan.

Ko, H. and Lee, K., 1987. "Automatic assembling procedure generation from mating conditions," *Computer Aided Design* 1987, Vol. 19, pp. 3-10.

Lee, K. and Nikolaidis, E., 1998. "Effect of member length on the parameter estimates of joints," *Computers and Structures*, Vol. 68, pp. 381-391.

Lotter, B., 1989. *Manufacturing Assembly Handbook*, Butterworths, London.

Malen, D. and Kikuchi, N., 1998. *Automotive Body Structure – A GM Sponsored Course in the University of Michigan*, ME599 Coursepack, University of Michigan.

Molloy, O., Tilley, S., and Warman, E. A., 1998. *Design for Manufacturing and Assembly*, Chapman & Hall, London.

Saitou, K. and Yetis, A., 2000. "Decomposition-based assembly Synthesis of structural products: preliminary results," *Proceedings of the Third International Symposium on Tools and Methods of Competitive Engineering*, April 2000, Delft, The Netherlands.

Yetis, A. and Saitou, K., 2000. "Decomposition-based assembly synthesis based on structural considerations," *Proceedings of the 2000 ASME Design Engineering Technical Conferences*, Baltimore, Maryland, September 10-13, DETC2000/DAC-1428.